2019

Effect of surface friction on ultrafast flame acceleration in obstructed cylindrical pipes

Abdulafeez Adebiyi

Rawan Alkandari

Damir Valiev

V'yacheslav Akkerman

Effect of surface friction on ultrafast flame acceleration in obstructed cylindrical pipes

Cite as: AIP Advances **9**, 035249 (2019); https://doi.org/10.1063/1.5087139
Submitted: 28 December 2018 . Accepted: 15 March 2019 . Published Online: 25 March 2019

Abdulafeez Adebiyi, Rawan Alkandari, Damir Valiev, and V'yacheslav Akkerman

Effect of surface friction on ultrafast flame acceleration in obstructed cylindrical pipes

Cite as: AIP Advances 9, 035249 (2019); doi: 10.1063/1.5087139
Submitted: 28 December 2018 • Accepted: 15 March 2019 •
Published Online: 25 March 2019

Abdulafeez Adebiyi,[1] Rawan Alkandari,[1] Damir Valiev,[2,3] and V'yacheslav Akkerman[1,a)]

AFFILIATIONS

[1]Center for Innovation in Gas Research and Utilization (CIGRU), Center for Alternative Fuels, Engines and Emissions (CAFEE), Computational Fluid Dynamics and Applied Multi-Physics Center, Department of Mechanical and Aerospace Engineering, West Virginia University, Morgantown, West Virginia 26506, USA

[2]Center for Combustion Energy, Key Laboratory for Thermal Science and Power Engineering of the Ministry of Education of China, Department of Energy and Power Engineering, Tsinghua University, Beijing 100084, China

[3]Department of Applied Physics and Electronics, Umeå University, 901 87 Umeå, Sweden

[a)]**Corresponding Author Email:** Vyacheslav.Akkerman@mail.wvu.edu

ABSTRACT

The Bychkov model of ultrafast flame acceleration in obstructed tubes [Valiev *et al.*, "Flame Acceleration in Channels with Obstacles in the Deflagration-to-Detonation Transition," Combust. Flame **157**, 1012 (2010)] employed a number of simplifying assumptions, including those of free-slip and adiabatic surfaces of the obstacles and of the tube wall. In the present work, the influence of free-slip/non-slip surface conditions on the flame dynamics in a cylindrical tube of radius R, involving an array of parallel, tightly-spaced obstacles of size αR, is scrutinized by means of the computational simulations of the axisymmetric fully-compressible gasdynamics and combustion equations with an Arrhenius chemical kinetics. Specifically, non-slip and free-slip surfaces are compared for the blockage ratio, α, and the spacing between the obstacles, ΔZ, in the ranges $1/3 \le \alpha \le 2/3$ and $0.25 \le \Delta Z/R \le 2.0$, respectively. For these parameters, an impact of surface friction on flame acceleration is shown to be minor, only 1~4%, slightly facilitating acceleration in a tube with $\Delta Z/R = 0.5$ and moderating acceleration in the case of $\Delta Z/R = 0.25$. Given the fact that the physical boundary conditions are non-slip as far as the continuum assumption is valid, the present work thereby justifies the Bychkov model, employing the free-slip conditions, and makes its wider applicable to the practical reality. While this result can be anticipated and explained by a fact that flame propagation is mainly driven by its spreading in the unobstructed portion of an obstructed tube (i.e. far from the tube wall), the situation is, however, qualitatively different from that in the unobstructed tubes, where surface friction modifies the flame dynamics conceptually.

I. INTRODUCTION

Among the geometries associated with fast flame acceleration and the deflagration-to-detonation transition (DDT) scenarios,[1–9] obstructed cylindrical tubes provide fastest acceleration.[10] While flame propagation through the obstacles is oftentimes associated with turbulence or shocks[11] or hydraulic resistance,[12] Bychkov *et al.*[13–16] identified a conceptually laminar, shockless mechanism of ultrafast acceleration in semi-open channels or cylindrical tubes equipped with a comb-shaped array of obstacles. The Bychkov mechanism is illustrated in Fig. 1, and it is devoted to a powerful jet-flow along the centerline of a channel or a tube, generated by a cumulative effect of delayed combustion in the "pockets" between the obstacles. According to the analytical formulation,[14] substantiated by the comprehensive numerical simulations,[14,17] a premixed flame front accelerates exponentially as $U_{tip}/S_L \approx \Theta \exp(\sigma\tau)$, where $U_{tip} \equiv dZ_{tip}/dt$ is the velocity of the flame tip in the laboratory reference frame, S_L is the unstretched laminar burning velocity, $\Theta \equiv \rho_f/\rho_b$ is the thermal expansion ratio, $\tau \equiv tS_L/R$ is the scaled time, R is the radius of the tube, and the scaled exponential acceleration rate σ in the cylindrical axisymmetric geometry is given by[14]

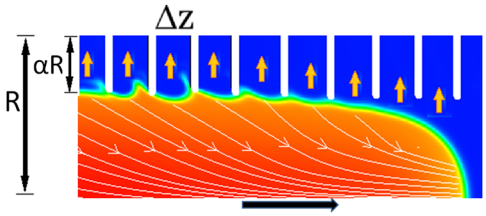

FIG. 1. The Bychkov mechanism of ultrafast flame acceleration in obstructed pipes (a half of the pipe is shown).

$$\sigma = \sigma(\Theta, \alpha) = 2\frac{(\Theta-1)}{(1-\alpha)}\left[1 + \frac{1}{2(\Theta-1)}\right], \tag{1}$$

where α is the blockage ratio. This acceleration is extremely powerful indeed, exceeding that due to wall friction[18] or combustion instabilities.[6] Moreover, the quantity σ grows with α and Θ, thereby promoting flame acceleration; σ drastically depends on α, but it does not depend on R, which makes this acceleration mechanism scale-invariant (Reynolds-independent) and, thereby, relevant to various scales: from micro-combustors to very large mining and subway tunnels.

The Bychkov model[13–17] adopted a set of simplifications, such as free-slip walls. However, slip walls are relevant for a non-continuum flow, while the physical boundary conditions are non-slip as far as the continuum assumptions are valid. Consequently, the Bychkov model needed to be validated in terms of its applicability to the practical reality. Indeed, it was shown that both surface friction[18] and thermal (cold and hot) wall conditions[19] play an enormous role in *unobstructed* pipes. Will it be the case in the obstructed ones? Here we are answering this question. While Ugarte *et al.*[16] have recently shown a *minor* effect of the outer isothermal walls as compared to the adiabatic ones, in obstructed pipes; in the present work we have compared slip and nonslip surfaces and came to the same conclusion.

II. NUMERICAL METHOD

We have performed the computational simulations of the hydrodynamic and combustion equations including transport processes (thermal conduction, diffusion, and viscosity), full compressibility and an Arrhenius chemical kinetics. The basic equations in the cylindrical geometry read:

$$\frac{\partial \rho}{\partial t} + \frac{1}{r}\frac{\partial}{\partial r}(r\rho u_r) + \frac{\partial}{\partial z}(\rho u_z) = 0, \tag{2}$$

$$\frac{\partial}{\partial t}(\rho u_r) + \frac{\partial}{\partial z}(\rho u_z u_r - \zeta_{zr}) + \frac{1}{r}\frac{\partial}{\partial r}\left[r\left(\rho u_r^2 - \zeta_{rr}\right)\right] + \frac{\partial P}{\partial r} + \frac{1}{r}\zeta_{\theta\theta} = 0, \tag{3}$$

$$\frac{\partial}{\partial t}(\rho u_z) + \frac{\partial}{\partial z}\left(\rho u_z^2 - \zeta_{zz}\right) + \frac{1}{r}\frac{\partial}{\partial r}\left[r(\rho u_z u_r - \zeta_{zr})\right] + \frac{\partial P}{\partial z} = 0, \tag{4}$$

$$\frac{\partial \varepsilon}{\partial t} + \frac{\partial}{\partial z}\left[(\varepsilon + P)u_z - \zeta_{zz}u_z - \zeta_{zr}u_r + q_z\right] + \frac{1}{r}\frac{\partial}{\partial r}\left[r\left((\varepsilon + P)u_r - \zeta_{rr}u_r - \zeta_{zr}u_z + q_r\right)\right] = 0, \tag{5}$$

$$\frac{\partial}{\partial t}(\rho Y) + \frac{1}{r}\frac{\partial}{\partial r}\left(r\rho u_r Y - r\frac{\mu}{\mathrm{Sc}}\frac{\partial Y}{\partial r}\right) + \frac{\partial}{\partial z}\left(\rho u_z Y - \frac{\mu}{Sc}\frac{\partial Y}{\partial z}\right) = -\frac{\rho Y}{\tau_R}\exp(-E_a/R_u T), \tag{6}$$

where Y is the mass fraction of the fuel mixture, $\varepsilon = \rho(QY + C_v T) + \rho\left(u_z^2 + u_r^2\right)/2$ is the total energy per unit volume, with the energy release in the reaction $Q = C_p T_f(\Theta - 1)$, specific heats at constant pressure and volume, C_p and C_v, pressure P, temperature T, density ρ and the radial and axial velocity components, u_r and u_z. Equation (6) describes a one-step irreversible Arrhenius reaction of the first order, with the activation energy E_a and the constant of time dimension τ_R. The stress tensor $\zeta_{\alpha\beta}$ is given by

$$\zeta_{rr} = \mu\left(\frac{4}{3}\frac{\partial u_r}{\partial r} - \frac{2}{3}\frac{\partial u_z}{\partial z} - \frac{2}{3}\frac{u_r}{r}\right), \quad \zeta_{zz} = \mu\left(\frac{4}{3}\frac{\partial u_z}{\partial z} - \frac{2}{3}\frac{\partial u_r}{\partial r} - \frac{2}{3}\frac{u_r}{r}\right), \tag{7}$$

$$\zeta_{\theta\theta} = \mu\left(\frac{4}{3}\frac{u_r}{r} - \frac{2}{3}\frac{\partial u_z}{\partial z} - \frac{2}{3}\frac{\partial u_r}{\partial r}\right), \quad \zeta_{rz} = \mu\left(\frac{\partial u_z}{\partial r} + \frac{\partial u_r}{\partial z}\right), \tag{8}$$

and the energy diffusion vector q_α takes the form

$$q_r = -\mu\left(\frac{c_P}{\mathrm{Pr}}\frac{\partial T}{\partial r} + \frac{Q}{\mathrm{Sc}}\frac{\partial Y}{\partial r}\right), \quad q_z = -\mu\left(\frac{c_P}{\mathrm{Pr}}\frac{\partial T}{\partial z} + \frac{Q}{\mathrm{Sc}}\frac{\partial Y}{\partial z}\right), \tag{9}$$

where $\mu \equiv \rho\nu$ is the dynamic viscosity, being $\mu_f = 1.7 \times 10^{-5}$kg/(m·s) in the fuel mixture, and Sc and Pr are the Schmidt and Prandtl numbers, respectively, with the Lewis number being their ratio, Le = Sc/Pr. To avoid diffusional-thermal instability, similar to Refs. 13–16, in the present work we took Le = Sc = Pr = 1. The fuel mixture has initial temperature, T_f = 300 K, pressure, P = 1 bar, and density, ρ_f = 1.16 kg/m^3. The thermal expansion ratio is taken to be Θ = 8, with the laminar flame speed being S_L = 0.347 m/s, which represents a near-stoichiometric methane-air mixture. The initial speed of sound in the fuel mixture is c_0 = 347 m/s, which exceeds S_L by a factor of 10^3, thereby making gasdynamics almost incompressible at the initial stage of burning, with the Mach number associated with flame propagation being $M_0 \equiv S_L/c_0 = 10^{-3}$. Then the thermal flame thickness can be defined, conventionally, as $L_f \equiv \mu_f/\rho_f S_L \mathrm{Pr} = 4.22 \times 10^{-5}$ m.

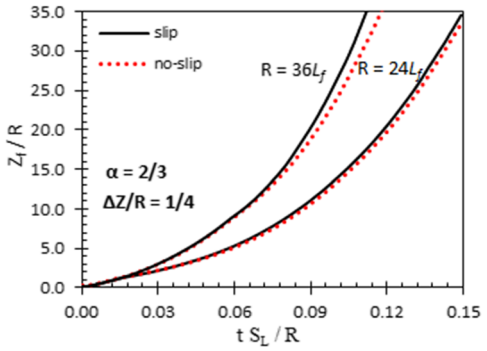

FIG. 2. The scaled flame tip position Z_f/R versus the scaled time $\tau \equiv tS_L/R$ for α = 2/3, $\Delta Z/R$ = 1/4, and various R = 24 L_f and 36 L_f.

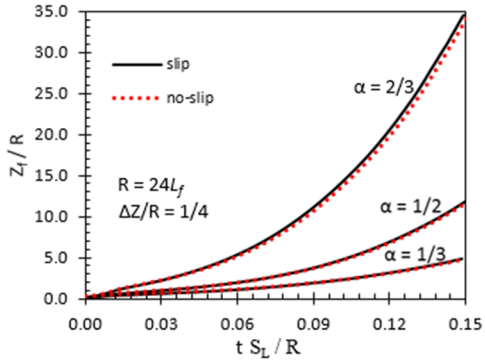

FIG. 3. The scaled flame tip position Z_f/R versus the scaled time $\tau \equiv tS_L/R$ for $R = 24\ L_f$, $\Delta Z/R = 1/4$, and various $\alpha = 1/3$, 1/2, and 2/3.

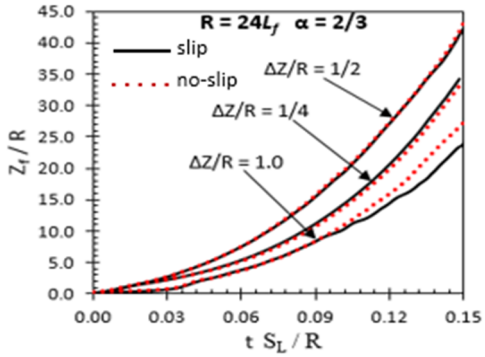

FIG. 6. The scaled flame tip position Z_f/R versus the scaled time $\tau \equiv tS_L/R$ for $R = 24\ L_f$, $\alpha = 2/3$ and various $\Delta Z/R = 1/4$, 1/2, and 1.

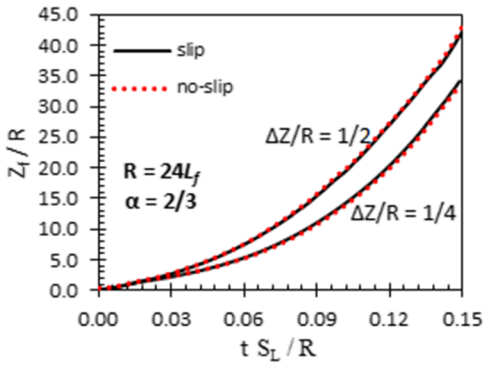

FIG. 4. The scaled flame tip position Z_f/R versus the scaled time $\tau \equiv tS_L/R$ for $R = 24\ L_f$, $\alpha = 2/3$ and various $\Delta Z/R = 1/4$ and 1/2.

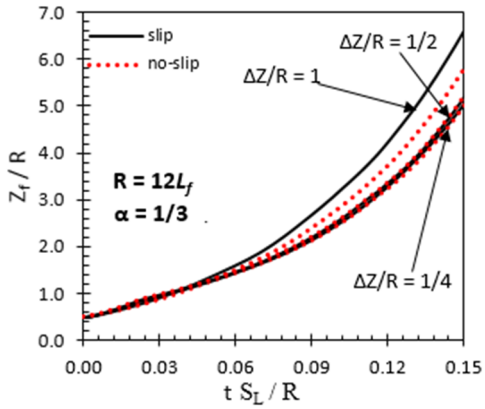

FIG. 7. The scaled flame tip position Z_f/R versus the scaled time $\tau \equiv tS_L/R$ for $R = 12\ L_f$, $\alpha = 1/3$ and various $\Delta Z/R = 1/4$, 1/2, and 1.

A flame propagates in a long cylindrical tube of radius R, with one end open, the blockage ratio α and the spacing between two neighboring obstacles ΔZ; see Fig. 1. This geometry is described by the Reynolds number associated with flame propagation, $\mathrm{Re}_f = RS_L/\nu = R/\mathrm{Pr}L_f = R/L_f$. In the present work, we used $\Delta Z/R = 1/4$, 1/2, 2; $\mathrm{Re}_f = 12$, 24; and $\alpha = 1/3$, 1/2, 2/3. We employed adiabatic, $\boldsymbol{n} \cdot \nabla T = 0$, and either free-slip, $\boldsymbol{n} \cdot \boldsymbol{u} = 0$, or non-slip, $\boldsymbol{u} = 0$, surfaces of the obstacles and of the pipe wall. Here $\boldsymbol{n}$ is a normal vector at a surface. The absorbing (non-reflecting) boundary conditions are adopted at the open end to prevent the reflection of the sound waves and weak shocks. The left end of the free part of the tube is blocked, while the right end is open, with the boundary conditions $\rho = \rho_f$,

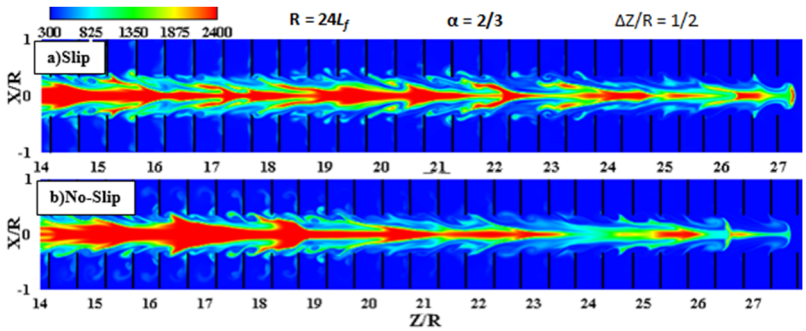

FIG. 5. The color temperature snapshots [in K] for burning in an obstructed tube with free-slip (a) and non-slip (b) walls for $R = 24\ L_f$, $\alpha = 2/3$, $\Delta Z = R/2$, and taken at the same scaled time instant $\tau = tS_L/R = 0.15$ in both cases.

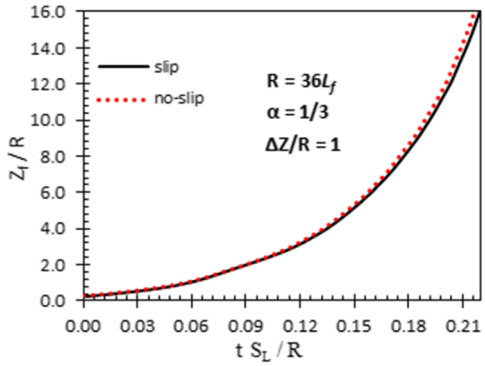

FIG. 8. The scaled flame tip position Z_f/R versus the scaled time $\tau \equiv tS_L/R$ for $R = 36\,L_f$, $\alpha = 1/3$, and $\Delta Z/R = 1$.

$P = P_f$, and $u_z = 0$ adopted there. The initial flame structure was imitated by a Zeldovich-Frank-Kamenetsky-like solution for a hemispherical flame front,[14] ignited at the centerline, at the closed end of the pipe. The computational grid consists of the 0.2 L_f × 0.2 L_f square cells; this resolution has been extensively tested for convergence in Ref. 14.

III. RESULTS AND DISCUSSION

We have compared the cases of free-slip and non-slip boundary conditions for various R, ΔZ, and α. Specifically, the scaled flame tip position Z_f/R versus the scaled time $\tau = tS_L/R$ is shown in Figs. 2–4, with the free-slip and non-slip boundary conditions depicted by the solid and dashed lines, respectively, in all plots. It is seen that the impact of free-slip and non-slip surface boundary conditions is minor as long as the obstacles spacing is small, $\Delta Z \le R/2$, and this is true for all α considered. Indeed, both the curves almost coincide in the cases studied. A reasonable way to measure a relative deviation between the plots is calculating the following quantity (in %):

$$E = \left|(Z_{f,slip} - Z_{f,no-slip})/Z_{f,no-slip}\right| \times 100. \quad (10)$$

The result of Eq. (10) does not exceed 1 ~ 4% for all the cases seen in Figs. 2–4; surface friction slightly moderates flame acceleration for $\Delta Z = R/4$, and very slightly promotes it for $\Delta Z = R/2$. This result certifies a minor impact of the free-slip/non-slip boundary conditions and thereby justifies the Bychkov model of flame acceleration

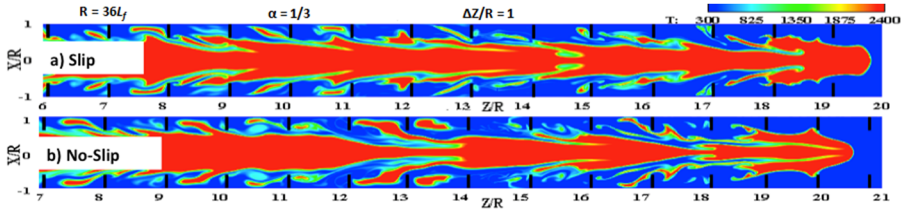

FIG. 9. The color temperature snapshots [in K] for burning in an obstructed tube with free-slip (a) and non-slip (b) walls for $R = 36\,L_f$, $\alpha = 1/3$, $\Delta Z/R = 1$ and taken at the same scaled time instant $\tau \equiv tS_L/R = 0.225$ in both cases.

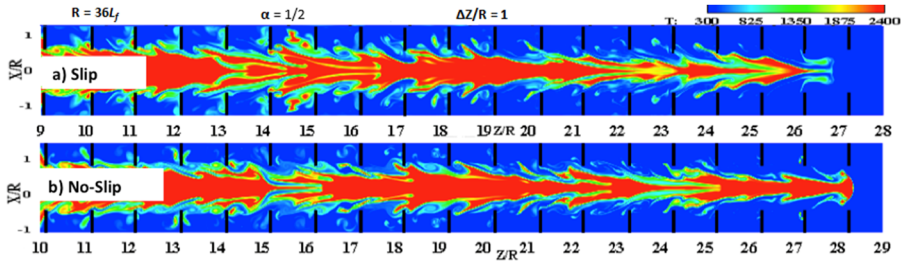

FIG. 10. The color temperature snapshots [in K] for burning in an obstructed tube with free-slip (a) and non-slip (b) walls for $R = 36\,L_f$, $\alpha = 1/2$, $\Delta Z/R = 1$ and taken at the same scaled time instant $\tau \equiv tS_L/R = 0.225$ in both cases.

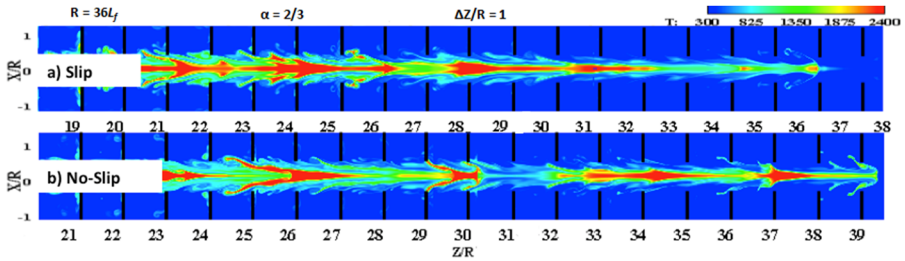

FIG. 11. The color temperature snapshots [in K] for burning in an obstructed tube with free-slip (a) and non-slip (b) walls for $R = 36\,L_f$, $\alpha = 2/3$, $\Delta Z/R = 1$ and taken at the same scaled time instant $\tau \equiv tS_L/R = 0.225$ in both cases.

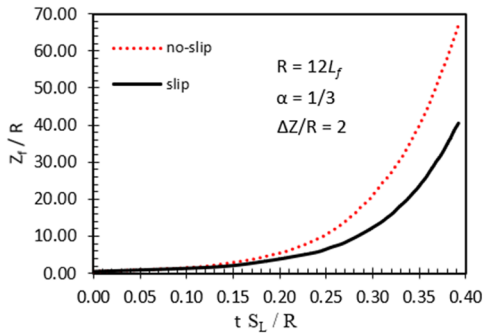

FIG. 12. The scaled flame tip position Z_f/R versus the scaled time $\tau \equiv tS_L/R$ for $R = 12\ L_f$, $\alpha = 1/3$, $\Delta Z/R = 2$.

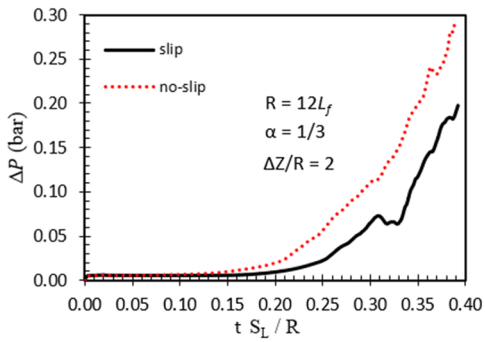

FIG. 13. Overpressure ΔP across the flame front taken at the flame tip versus the scaled time $\tau \equiv tS_L/R$ for $R = 12\ L_f$, $\alpha = 1/3$, $\Delta Z/R = 2$.

in obstructed pipes, which employs the free-slip surfaces of obstacles and walls. The similarity of the color snapshots of Fig. 5 taken at the scaled time instant $\tau = 0.15$ leads to the same conclusion. This result can be explained by the fact that the flow is mainly driven in the axial direction such that the small obstacles spacing mitigates a potential effect of surface fiction (if any). In fact, Ref. 16 suggested the same conclusion with the same explanation when studying the thermal boundary conditions at the walls and obstacles in obstructed channels.

We also investigated what happened when the obstacles spacing is increased. While in Figs. 6–8 we noticed that the results for both free-slip and non-slip conditions almost coincide for a small ΔZ, $\Delta Z \le R/2$, as discussed previously, the difference between the results is observed when $\Delta Z = R$. Additionally, the color snapshots have been taken at time scaled instant $\tau = 0.225$ from the simulations for the free-slip and non-slip boundary conditions, as presented in Figs. 9–11. It is seen that there is only a minor difference between the free-slip and non-slip surfaces, with the flame tip being ~1.5 R ahead for the non-slip case. This result can potentially be attributed to the fact that vortices in the pockets are barely in contact with the walls.

We have also considered a wider spacing between the obstacles, $\Delta Z = 2R$, with a remarkable difference between the free-slip and non-slip conditions observed in that case, as shown in Figs. 12–15. Specifically, the time evolutions of the flame tip positions Z_f and of the overpressures ΔP across the flame front, taken at the flame tip, are shown in Figs. 12 and 13, respectively. Figures 14 and 15 compare the color representations for the vorticity, Fig. 14, and temperature, Fig. 15. It is clearly seen that surface friction promotes flame acceleration, substantially, as compared to the free-slip condition: the deviation given by Eq. (10) is ~24% in that case. Comparing Fig. 14b to 14a, one can attribute such a discrepancy to the formation of high vorticity in the pockets between the obstacles in the case if large ΔZ. Obviously, vorticity evolves differently with free-slip and non-slip surfaces, with a stronger flow distortion in the latter case, leading thereby to faster flame acceleration. It is recalled, in this respect, that the Bychkov model does not consider vorticity and, therefore, it is probably not fully applicable here. Moreover, the very approach of tightly-packed obstacles, $\Delta Z \ll R$, Fig. 1, considered in the Bychkov model, is definitely broken when ΔZ exceeds R. In fact, an inapplicability of the Bychkov formulation for $\Delta Z > R$ has been shown even in the pilot studies[13,14] as well as later, in the detailed analysis.[16] Qualitatively, we arrive to the same conclusions by means of the color snapshots in Fig. 15. Indeed, while a resemblance between Figs. 5a and 5b was evident, with the flame tip at $Z_f \sim 27\ R$ in both figures, a serious difference between the flame tip positions in Figs. 15a and 15b is clearly seen, with the flame tip being ~19 R ahead for the non-slip case.

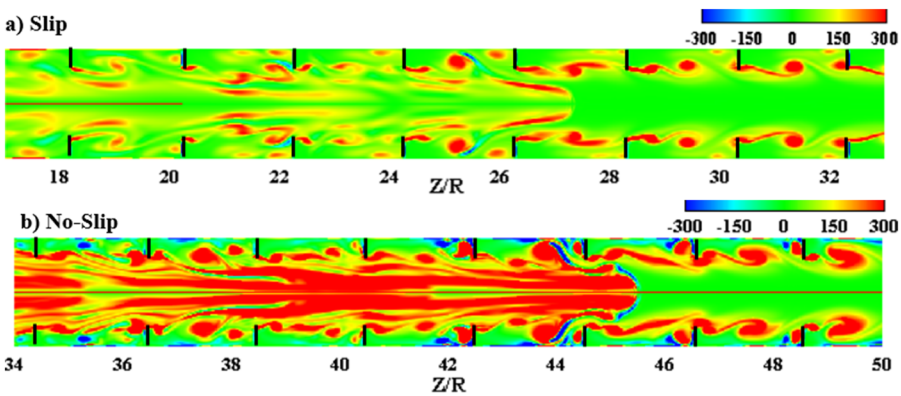

FIG. 14. The color θ-vorticity snapshots [in sec $^{-1}$] for burning in an obstructed tube with free-slip (a) and non-slip (b) walls for $R = 12\ L_f$, $\alpha = 1/3$, $\Delta Z/R = 2$ and taken at the same scaled time instant $\tau \equiv tS_L/R = 0.36$ in both cases.

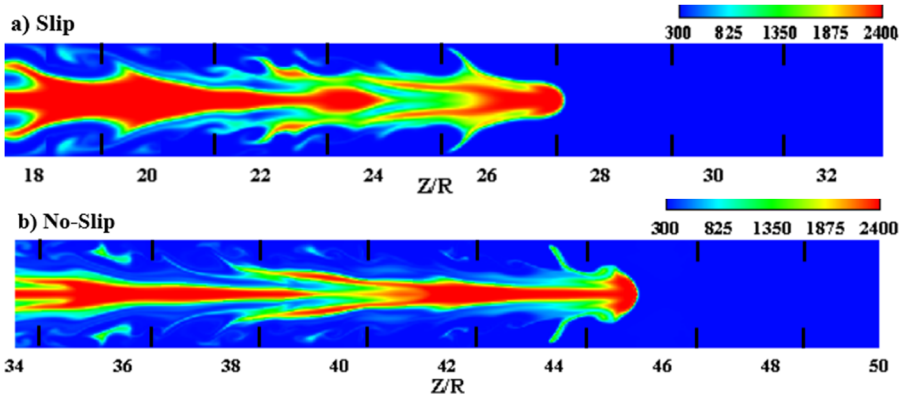

FIG. 15. The color temperature snapshots [in K] for burning in an obstructed tube with free-slip (a) and non-slip (b) walls for $R = 12\ L_f$, $\alpha = 1/3$, $\Delta Z/R = 2$ and taken at the same scaled time instant $\tau \equiv tS_L/R = 0.36$ in both cases.

IV. CONCLUSIONS

We have investigated flame propagation in obstructed cylindrical tubes. It is shown that for small and moderate spacing between the obstacles, an impact of surface friction on flame acceleration is minor, 1~4%, slightly facilitating acceleration in a tube with $\Delta Z/R = 1/2$ and moderating acceleration in the case of $\Delta Z/R = 1/4$. However, the situation is different in the case of a wide spacing. Earlier, a minor effect of the isothermal surfaces as compared to the adiabatic ones was also demonstrated.[16] With the fact that the Bychkov model employed slip walls whereas the physical boundary conditions are non-slip as far as the continuum assumption is valid, the present work thereby justifies the Bychkov approach and makes its wider applicable to the practical reality; but only within its validity limit. Indeed, at a large spacing, $\Delta Z \gg R$, the Bychkov model is not applicable anyway, and vorticity comes to play and show different behaviors for the free-slip and non-slip surfaces. In fact, we anticipated such an outcome that the effect of surface friction is generally minor (but only as long the spacing between the obstacles is small). It can be explained by a fact that flame propagation is mainly driven by its spreading in the unobstructed portion of an obstructed tube (i.e. far from the tube wall). However, there was a need to justify this hypothesis because surface friction may potentially play a significant role as it does in other geometries such as unobstructed tubes.[18] Here we proved this is not the case for an obstructed tube.

ACKNOWLEDGMENTS

V'yacheslav Akkerman was sponsored by the U.S. National Science Foundation (NSF), through his CAREER Award #1554254, and by the West Virginia Higher Education Policy Commission (WV HEPC) through the Grant #HEPC.dsr.18.7. Damir Valiev was supported by the National Science Foundation of China (NSFC), through the Grant #51750110503, and by the Thousand Young Talents Plan Program.

REFERENCES

[1]G. D. Roy, S. M. Frolov, A. A. Borisov, and D. W. Netzer, "Pulse detonation propulsion: Challenges, current status, and future perspective," Prog. Energy Combust. Sci. **30**, 545–672 (2004).
[2]S. B. Dorofeev, "Flame acceleration and explosion safety applications," Proc. Combust. Inst. **33**, 2161–2175 (2011).
[3]M. H. Wu, M. P. Burke, S. F. Son, and R. A. Yetter, "Flame acceleration and the transition to detonation of stoichiometric ethylene/oxygen in microscale tubes," Proc. Combust. Inst. **31**, 2429–2436 (2007).
[4]J. D. Ott, E. S. Oran, and J. D. Anderson, "A mechanism for flame acceleration in narrow tubes," AIAA Journal **41**, 1391–1396 (2003).
[5]L. Kagan and G. Sivashinsky, "On the transition from deflagration to detonation in narrow tubes," Flow, Turbul. Combust. **84**, 423–437 (2010).
[6]D. Bradley, C. G. W. Sheppart, R. Woolley, D. A. Greenhalgh, and R. D. Lockett, "The development and structure of flame instabilities and cellularity at low Markstein numbers in explosions," Combust. Flame **122**, 195–209 (2000).
[7]Q. Li, X. Sun, S. Lua, Z. Zhang, X. Wang, S. Han, and C. Wang, "Experimental study of flame propagation across a perforated plate," Int. J. Hydrogen Energy **43**, 8524–8533 (2018).
[8]D. A. Kessler, V. N. Gamezo, and E. S. Oran, "Simulations of flame acceleration and deflagration-to-detonation transitions in methane-air systems," Combust. Flame **157**, 2063–2077 (2010).
[9]B. Zhang, H. Liu, and C. Wang, "On the detonation propagation behavior in hydrogen-oxygen mixture under the effect of spiral obstacles," Int. J. Hydrogen Energy **42**, 21392–21402 (2017).
[10]E. S. Oran and V. N. Gamezo, "Origins of the deflagration-to-detonation transition in gas-phase combustion," Combust. Flame **148**, 4–47 (2007).
[11]G. Ciccarelli and S. Dorofeev, "Flame acceleration and transition to detonation in ducts," Prog. Energy Combust. Sci. **34**, 499–550 (2008).
[12]I. Brailovsky, L. Kagan, and G. Sivashinsky, "Combustion waves in hydraulically resisted systems," Philos. Trans. R. Soc. A **370**, 625–646 (2012).
[13]V. Bychkov, D. Valiev, and L.-E. Eriksson, "Physical mechanism of ultrafast flame acceleration," Phys. Rev. Lett. **101**, 164501 (2008).
[14]D. Valiev, V. Bychkov, V. Akkerman, C. K. Law, and L.-E. Eriksson, "Flame acceleration in channels with obstacles in the deflagration-to-detonation transition," Combust. Flame **157**, 1012–1021 (2010).
[15]V. Bychkov, V. Akkerman, D. Valiev, and C. K. Law, "Influence of gas compression on flame acceleration in channels with obstacles," Combust. Flame **157**, 2008–2011 (2010).
[16]O. Ugarte, V. Bychkov, J. Sadek, D. Valiev, and V. Akkerman, "Critical role of blockage ratio for flame acceleration in channels with tightly spaced obstacles," Phys. Fluids **28**, 093602 (2016).
[17]V. Akkerman and D. Valiev, "Moderation of flame acceleration in obstructed cylindrical pipes due to gas compression," Phys. Fluids **30**, 106101 (2018).
[18]V. Bychkov, A. Petchenko, V. Akkerman, and L.-E. Eriksson, "Theory and modeling of accelerating flames in tubes," Phys. Rev. E **72**, 046307 (2005).
[19]V. N. Gamezo and E. S. Oran, "Flame acceleration in narrow tubes: Effect of wall temperature on propulsion characteristics," 44th AIAA Aero. Sci. Meeting & Exhibit, Reno, NV, Jan 9-12, 2006.